NANOSYSTEMS: PHYSICS, CHEMISTRY, MATHEMATICS, 2013, 4 (5), P. 680–689

NANOSCALE STRUCTURES BASED ON THE $Zn_{1-x}Cd_xS$

M. A. Jafarov, E. F. Nasirov

Baku State University, Baku 1045, Z.Khalilov st.23, Azerbaijan

maarif.jafarov@mail.ru

PACS 73.20.-e; 78.66.Hf; 68.55.-a

In this work, the results of the investigation of the precularity near the solar spectrum region, of $Zn_{1-x}Cd_xS$ nanoparticles, nanofilms, nanoscale p-n and heterojunction prepared on glass-ceramic and alumminium substrates by precipitation from aqueous solutions are presented. We investigated the preparation of ZnCdS nanoparticles in a micro-emulsion system stabilized with nonionic surface active materials, as well as the impact of drop volume and supersaturation the size of the formed ZnCdS particles. The temperature dependence of dark and light conductivity, spectrum and optical quenching of primary and impurity photoconductivity were investigated. Direct current-voltage characteristic structure of Al/p-CdS/n-CdS is almost identical to the current-voltage characteristics of p-n junctions. Volt-farad characteristics of the samples established the presence of conduction due to the presence of reverse bias p-n junctions. In the following order, CdTe/CdS/$Zn_{1-x}Cd_xS$ structure have 75% or slightly higher quantum efficiency in the 400–850 nm wavelength region.

Keywords: chemical bath deposition, nanoparticle, nanoscale p-n junction, micro emulsion system.

1. Introduction

Among the many different methods available to deposit films of semiconductors, chemical bath deposition (CBD) must rank as the simplest conceptually [1–3]. CBD refers to depositions from solution (usually aqueous) where the required deposit is both chemically generated and deposited in the same bath [4–7]. Thus, deposition from a supersaturated solution or spin coating from a colloidal sol are not included under the aegis of CBD: in both cases, the layer material must be pre-prepared. Neither is sol-gel layer formation, although it could be reasonably argued that the cross-linking which occurs during the process constitutes a chemical reaction. Successive ion layer adsorption and reaction (SILAR) is a related technique, where a substrate is first dipped in an ionic solution of one component, rinsed, then dipped in a solution of the second component and rinsed; this ideally results in a single monolayer of the desired compound [8–10]. Liquid phase deposition (LPD) is a specific subset of CBD often used for acidic oxides. In spite of it being so simple, it is one of the least known. If scientists or engineers in general would be asked to name some semiconductor film deposition methods, evaporation, chemical vapor deposition, sputtering, perhaps even electrodeposition, would be the most obvious techniques that would come to mind: CBD would probably be lower on the list (with the obvious exception of those who work with the method). Part of the reason is the many different terms which are used to denote CBD: chemical solution deposition (previously more popular, but a consensus is beginning to favor the use of CBD), chemical deposition (when it is clear that chemical vapor deposition — a very different technique — is not meant) and liquid phase deposition [11–13].

In the last decade the interest in nano-objects with specific features is sharply increased. This interest is related to the unique properties of nanoparticles, which differ from

that of normal-size particles. The investigation nanoparticle properties is one of the main aims of the novel directions for physical chemistry. Developing of this direction is closely related with the methods of synthesis, which allow the preparation of nanoparticles having the required size and rather narrow size distribution. The reverse micro emulsion systems are thermodynamically sustainable double phase systems, which consist of polar phase micro drops, distributed in nonpolar ambient. Surface-active materials (SAM) are used to stabilize systems like this. This allows one to perform chemical reactions among materials in polar phase and forming sparingly-soluble compounds. The advantage of this nanoparticle preparion method is its relative simplicity and also the possibilities of simultaneous synthesis and stabilization of the prepared particles [14].

The obtained results show that when controlling ionic composition and heat treatment (HT) conditions, one can control the properties of $Zn_{1-x}Cd_xS$ films. Furthermore, the above films are similar in their main photoelectric properties and parameters to such model crystals as CdS and ZnS, to allow for the effect of sticking centers, conditioned polycrystalline structure. $Zn_{1-x}Cd_xS$ films can be used as photodetectors of the near IR region. The purposes of these investigations are to determine the general regularities and characteristic of recombination and electron-molecular processes, determinant high sensitivity in the IR region, versus the composition and HT conditions, the photoelectrical properties of $Zn_{1-x}Cd_xS$ ($0 \leqslant x \leqslant 0.6$) films deposited from the solution. Until recently, converters based on CdS were produced mainly as a heterostructure. Creation of a p-n junction is difficult because of the receipt of CdS with hole conductivity. The literature contains little data concerning the single-crystal film-p-n-junction. In this paper, we present the results for studies of nanoscale p-n junction based on solution-precipitated CdS. The samples were prepared by precipitation from solution onto an aluminum substrate. Before applying the lower aluminum electrode, the sample was kept in air at 300 $^\circ$C, for 10 min. Based on the measurement of current-voltage (I-V), capacitance-voltage (C-U), and thermally stimulated conductivity (TSC) characteristics of the samples, it was established that conductivity exists due to the presence of p-n junctions.

In the solar cell of CdTe, the lattice mismatch between n-CdS and p-CdTe and the low bandgap of CdS window layer are known to have some drawback on cell performance. By using higher bandgap materials, like ZnS or $Zn_{1-x}Cd_xS$ as a heterojunction partner to CdTe, one can improve the window bandgap, but the lattice mismatch of these materials is worse than that of CdS. Trading off the latter mismatch for the higher bandgap may not be the solution, for the loss in cell performance due to lattice mismatch outweighs the gain due to the increase in window bandgap. Therefore, to retain the compatibility of CdS and CdTe and still improve the short wavelength spectral response of CdTe solar cell, its traditional CdS/CdTe structure should be changed to $Zn_{1-x}Cd_xS$/CdTe. In other words, a $Zn_{1-x}Cd_xS$/CdS layer should replace the CdS-only window layer.

2. Experiment

In this paper we investigated the preparation of ZnCdS nanoparticles in a a nonionic surfactant-stabilized micro emulsion as well as the impact of drop volume and supersaturation on the size of the formed ZnCdS particles. Hexamethylene was used as the non polar phase, while water, aqueous solutions of $Cd(Ac)_2$, $ZnCl_2$ and precrystallized $Na_2S_20_3$ were used as the polar phase.

All solutions were prepared in doubly-distilled water. Reverse micro emulsion systems were prepared by the solubilization of water, aqueous solutions according to salts in a reverse micellar system, in which the Tx-100 concentration was 0.3 M and SAM/n-SAM ratio was

4:1. The water or aqueous solutions of the corresponding salts were added to a defined volume of this solution with drops in such amount that the W=[H_2O] /[SAM] ratio was varied from 5–15. Equal volumes of the micro emulsion with similar content, containing ions of the reacting substances in aqueous phase were mixed for preparing cadmium sulfide.

The particle size of the prepared cadmium sulfide was determined by a spectrophotometric method. The dependence of optical density on the wavelength was measured by a spectrophotometer in a cuvette from 320–900 nm.

The $Zn_{1-x}Cd_xS$ ($0 \leqslant x \leqslant 0.6$) films of 0,03–2 μm thickness were deposited on glass ceramic substrates from an aqueous solution by the method described previously [3]. The thicknesses of the p-CdS, CdTe and $Zn_{1-x}Cd_xS$ ($0 \leqslant x \leqslant 0.6$) films were obtained using a Dektak profilometer. Transmission measurements were performed using a spectrophotometer.

This was prepared by adding into the beaker containing the stirred deionized water at 85 $^\circ$C, $Cd(OAc)_2$, $Zn(OAc)_2$, NH_4OH, and $Na_2S_2O_3$, from 0.05, 0.05, 12 and 0,2 M stock solutions, respectively, in that order.

Since the CBD-grown CdS layer has produced some of the best performing cells, the growth of the new $Zn_{1-x}Cd_xS$/CdS window layer by CBD should therefore be explored. Each experimental solution contained 300 ml of deionized water.

The nanofilm's composition ($0 \leqslant x \leqslant 0.6$) was changed by the partial substitution of the thiourea and was controlled by chemical, spectral and X-ray phase analyses. XRD pattern of $Zn_{1-x}Cd_xS$ thin films results are shown in Fig.1 a,b. The results for the spectral dependence of the optical transmittance of $Zn_{1-x}Cd_xS$ films are shown in Fig. 2. Sections of the films were subjected to aerobic HT at temperatures of 400–500 $^\circ$C for 0–30 min.

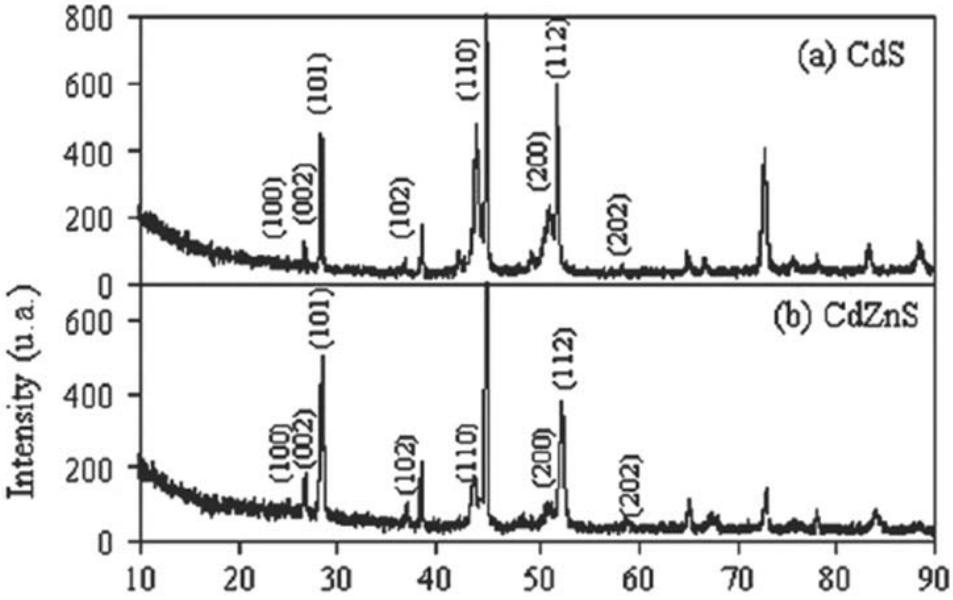

Fig. 1. XRD pattern of thin films: (a) CdS, (b) ZnCdS

The morphologies of the products were observed by SEM. These images clearly indicate that the products are spherical. It can also be seen that there is a uniform size distribution in all products. Figure 2 shows the scanning electron microscopy (SEM) micrographs for the films deposited and annealed at various temperatures. The SEM micrograph of the films deposited at a higher bath temperature, such as 80 $^\circ$C, in the miroemulsion system is shown in Fig. 2a. No pinholes can be observed for these films. The films show

more grain formation and well defined particle edges. However, there seems to be a slight decrease in the number of grains for the films annealed at 200, 300 and 500 ° C. The surface of the substrate is not covered completely at these bath temperatures. The grain formation was observed as an irregular agglomeration with the grain sizes completely different from one another (2–5 μm). These observations suggest an incomplete nucleation step with an irregular grain growth rate. This is due to coating of inorganic core by the surfactant, which prevents the nanoparticle aggregation. It has been proven that the prevention of nanoparticle aggregation in the presence of a surfactant is more effective when the surfactant has a long and branched chain structure. Fig. 3. shows the distribution of nanoparticles ZnCdS.

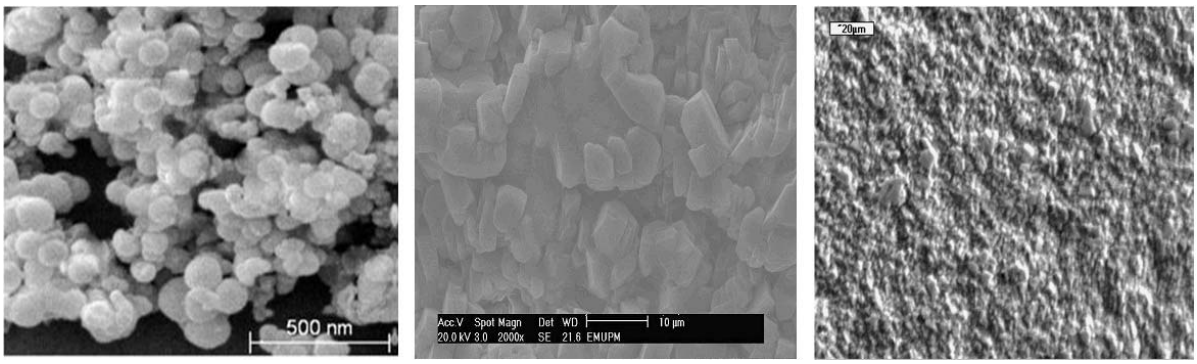

FIG. 2. SEM micrographs of Zn_{1-x} Cd_xS films deposited at higher bath temperature such as 80 ° C in miroemulsion sistem (1) and annelaited at different temperatures, 2—300 ° C, 3—500 ° C

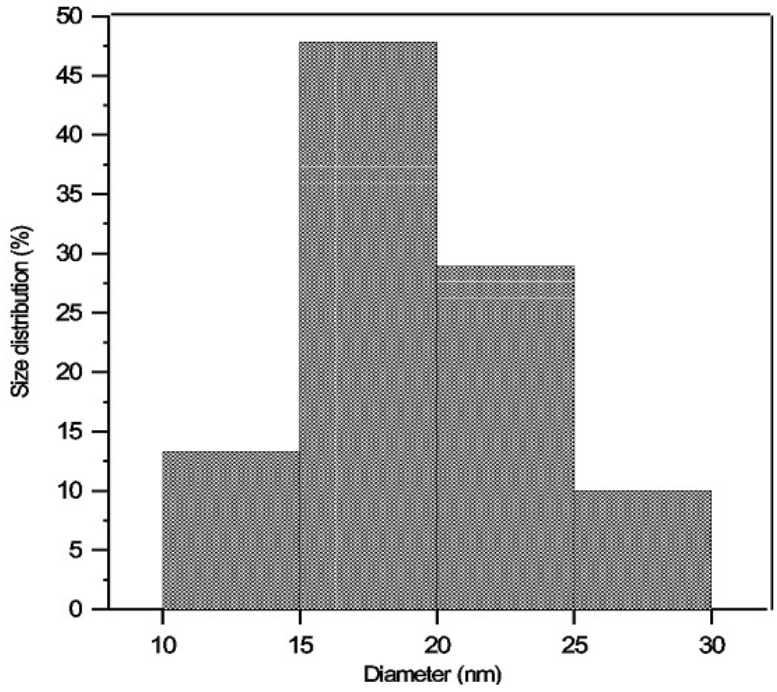

FIG. 3. Distribution nanoparticles Zn CdS

The temperature dependence of dark (σ_{dk}) and light conductivity (σ_{ph}), the spectrum and optical quenching of photoconductivity (σ_{oq}), the current-illumination characteristics,

and the thermostimulated conductivity from 80–400 K were investigated. According to the thermopower measurements, the films were n-type. The dark conductivity of Zn_{1-x} Cd_xS films was found to vary with x, from 10^{-4} to 10^{-5} S/cm.

The ratio of photocurrent to the dark current reached 10^2 to 10^3. The carrier concentration determined from Hall measurements was $3–5\times10^{14}$ cm^{-3} and 10^{16} cm^{-3} for the films with x=0 and x=0.3, respectively. The spectral dependence of optical transmittance of $Zn_{1-x}Cd_xS$ films is shown in Fig. 4.

Just after deposition, the above films were characterized by long-term relaxation photoeffects. Subsequent to heat-treatment, considerable changes in the photoelectric (PE) properties versus the composition, temperature and annealing time (τ_a) were observed. The dependence of conductivity as a function of time (τ_0) has a nonmonotonic character, i.e. with low τ_a, the conductivity of films increases and achieves a maximum value exceeding the initial one by more than four orders of magnitude. Further increase of the annealing time up to 15 min leads to a sharp decrease in the conductivity.

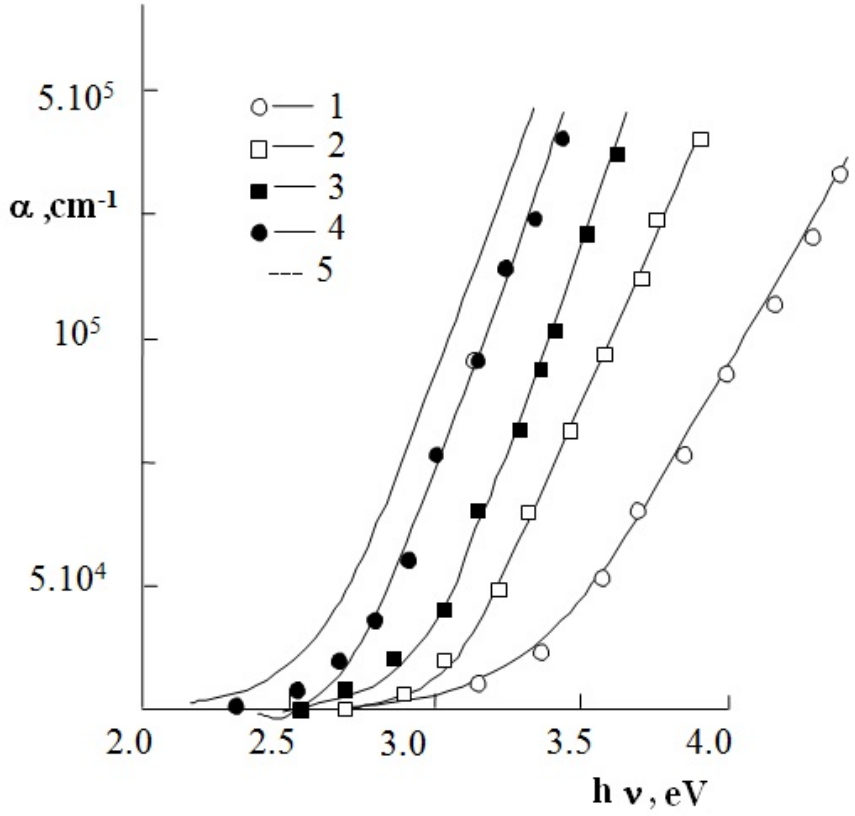

FIG. 4. The spectral dependence of optical transmittance of $Zn_{1-x}Cd_xS$ films.
X=: 1—0.1, 2—0.3, 3—0.5, 4—0.7, 5—0.9

The $\sigma_c(\tau_a)$ dependence has an extremum character, i.e. primarily it increases for annealing times up to 15 min, then (t$\geqslant$15 min), a slow decay is observed. With increased annealing temperatures and x, a shift of the above dependence extrema toward lower times takes place. A photoconductivity spectrum maximum of $Cd_{1-x}Zn_xS$ ($0\leqslant x\leqslant0.6$) films was observed at 0.445–0.495 μm versus the composition. Subsequent to heat treatment, the photoconductivity spectrum considerably widened and the peaks at (0.58–0.70) μm and (0.90–1.13) μm appeared. With increased time, to $4\leqslant \tau_a \leqslant15$ min, the intensities of additional maxima increased and the intensity of the principal maximum decreased. The $Cd_{1-x}Zn_xS$

($0 \leqslant x \leqslant 0.6$) films after the heat treatment at 500 ° C for 5–10 min exhibited high sensitivity ($\sigma_{ph}/\sigma_{dk} = 10^7$ to 10^8) over a wide spectral range.

The research of I-U, C-U characteristics and thermally stimulated conductivity from 80–400 K was performed. The I-U was removed in a pulsed, static and dynamic mode and the C-U characteristics by the use of a RLC bridge, allowing simultaneous measurement of the barrier capacitance and the differential resistance of the barrier, as well as resistance in the neutral part of the semiconductor. Volt-ampere characteristic (VAC) nanoscale p-n transition p-CdS/n-CdS has rectifying properties by a factor of 10^3–10^4 with a voltage of $U = 1.5 \div 2$ B (Fig. 5). It is shown that the barrier width is 100 nm at zero bias and reaches 150 nm at a voltage of 2 V reverse mixing.

Below 250 K, the slope remains almost constant, which corresponds to the dominant role of tunneling processes, and above 250 K, with increased temperature the slope increases, indicating the growing role of thermal processes. Direct parts of the VAC (in logarithmic scale) consist of two parts, corresponding to different mechanisms of current flow.

We have demonstrated using chemical and thermal activated diffusion that $Zn_{1-x}Cd_xS$ thin films can be synthesized from electrochemically-deposited ZnS/CdS multilayers. A more homogeneous $Zn_{1-x}Cd_xS$ film is obtained at lower processing temperatures if the stacked layers are thin. It is of great importance that the grown structure is almost homogenized in the chemical bath at temperatures below 90 ° C. The homogenization of our structure was achieved by annealing at 400 ° C, the temperature generally used for processing solar cells. The low processing temperature developed here in the fabrication of $Zn_{1-x}Cd_xS$ means that the proposed $Zn_{1-x}Cd_xS$/CdS solar cell window could be grown at temperatures that will not damage the glass or the underlying transparent conducting oxide generally used as a substrate in solar cells.

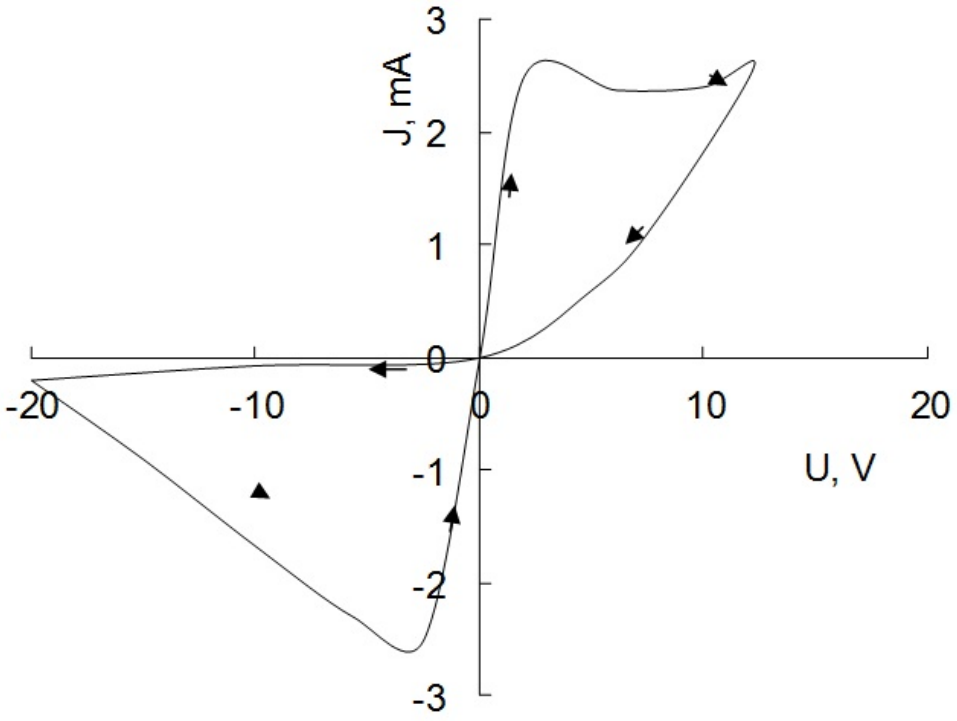

FIG. 5. VAX p-n junction based on CdS

To achieve the new $Zn_{1-x}Cd_xS/CdS$ structure proposed for the CdTe window layer, what is required is simply an additional growth of CdS on top of the $Cd_{1-x}Zn_xS$ layer obtained from a chemical deposition ZnS/CdS multilayer.

The structures are Al/p-CdTe/$Zn_{1-x}Cd_xS$/contact, type 1 Al/CdTe/CdS/$Zn_{1-x}Cd_xS$ and type 2 Al/p-CdS/CdTe/$Zn_{1-x}Cd_xS$ (Fig. 6).

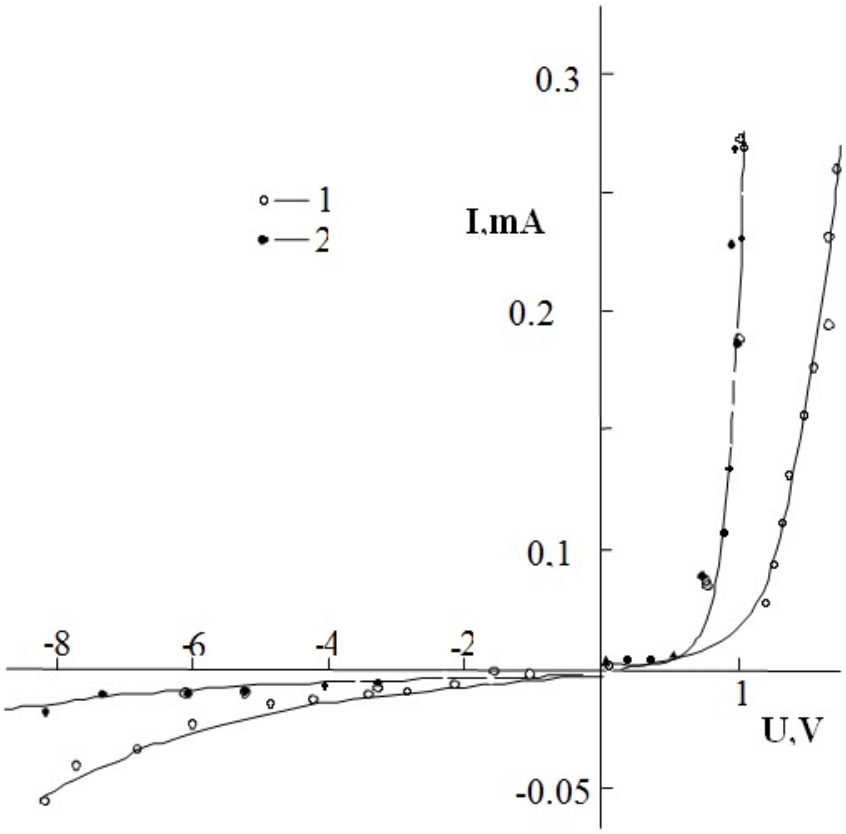

FIG. 6. VAX structures Al/CdTe/CdS/$Zn_{1-x}Cd_xS$ (1) and Al/p-CdS/CdTe/$Zn_{1-x}Cd_xS$ (2)

The sample was then annealed in $CdCl_2$/Ar ambient (75% $CdCl_2$+ 25% Ar) at 400 ° C for 15 min. The window fabrication was completed by the deposition of an additional 0.35 μm-thick p-CdS film. In the following order, CdTe/p-CdS/$Zn_{1-x}Cd_xS$ structure have 75% or slightly higher quantum efficiency in the 400–850 nm wavelength region (Fig. 7). We note that the structure with the $Zn_{1-x}Cd_xS$ layer generally has a better short wavelength response, than the expected value.

3. Discussion of results

Interpretation of the experimental results becomes complicated due to the simultaneous occurrence of several processes (evaporation, generation and transformation of intrinsic defects) which arise in films during heat treatment. The kinetics of every process has a complicated character [5]. The dependence observed in photoelectric properties of films point out the changes of concentration of defects of donor and (or) acceptor character due to film annealing. Decreases of film photosensitivity at shorter annealing times (τ_a) indicated an increase in the concentration of fast-recombination centers (s-centers), i.e. the increase of

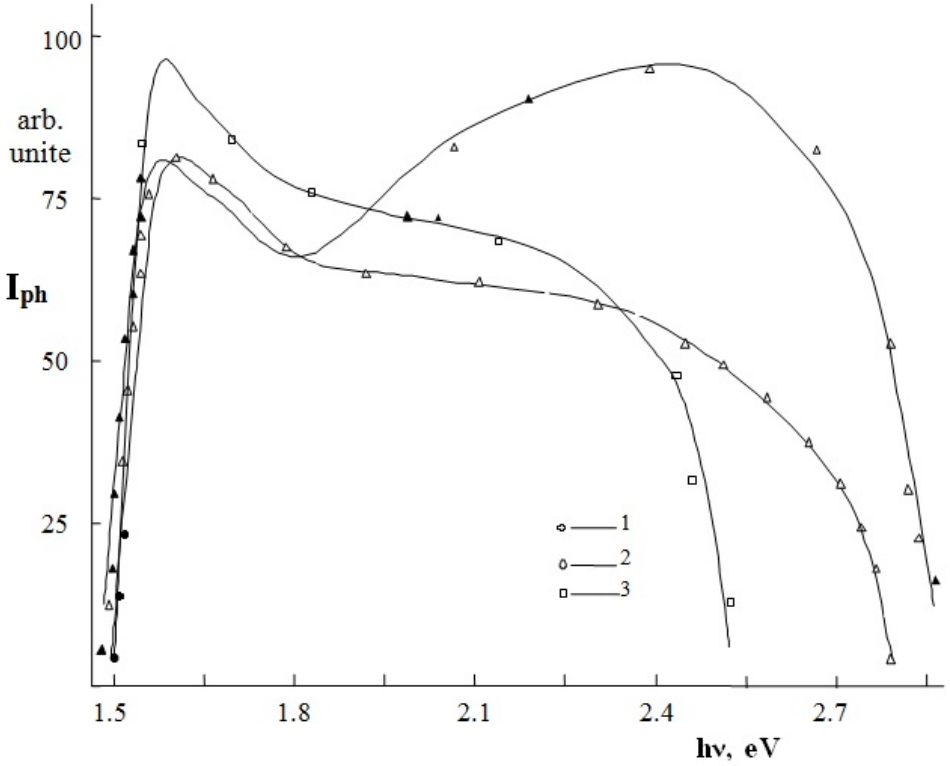

FIG. 7. Spectral response of the photocurrent through Zn_{1-x} Cd_xS ($0 \leqslant x \leqslant 0.6$) films annealed in air at 500 ° C for (1) 0, (2) 5, (3) 15 min

the recombination flux (g_s), and hence the decrease in the life of electrons takes place. Measurements of the current- illumination characteristics of the samples showed that at shorter annealing times the decrease in hole concentration on the slow recombination centers (r-centers) was observed. This fact can be attributed either to an increase of the compensating shallow donor concentration or a decrease of the r-center concentration. A simultaneous increase in the concentration of the shallow donor centers is responsible for the increased dark conductivity and the fast recombination centers, causing decreased photosensitivity, allowing us to assume that the s-centers are complexes consisting of shallow donors [9].

The change observed at $\tau_a \geqslant 5$ min can be explained when the anion and the cation vacancies diffuse into the volume are formed on their surfaces. Due to heavy evaporation of metal during initial stages of annealing, the near-surface region is mainly enriched by cadmium and sulfur vacancies playing the role of slow recombination centers. Their diffusion into the volume leads to an increased photosensitivity and to decreased dark conductivity. In this case, the complexes of cadmium, sulfur and selenium vacancies, i.e. the recombination r-centers, were formed.

The decreased photoconductivity for annealing times $\tau_a > 15$–20 min is attributed to a single electron-molecular mechanism considering the initial state of the film surface as well as the local and collective phenomena during chemisorption. In the initial state of annealing, the increased surface potential barrier due to chemisorption leads to an increase of the film sensitivity due to slow recombination. When the recombination was controlled by r-centers, the increase in their occupancy by holes due to chemisorption resulted in a decrease of the photoholes' lifetime, i.e. the photoconductivity decreased. In this case, with increased sulfur concentration in films the effect of oxygen became lower.

The obtained results showed that when controlling the ionic composition and HT conditions, one can control the properties of $Zn_{1-x}Cd_xS$ ($0 \leqslant x \leqslant 0.6$) films, achieving the appropriate degree of compensation of recombination levels and traps attributed to the intrinsic defects or impurities. In this way, model crystals, such as CdS and ZnS, can explain the main photoelectrical properties and parameters of $Zn_{1-x}Cd_xS$ ($0 \leqslant x \leqslant 0.6$) films.

Hence, the space charge region in the investigated structures is only part of the film thickness and the space charge region in p-CdS is very narrow, due to the sharp asymmetry of the conductivity. In the beginning, the external voltage drops on the space charge region in CdS n-type. The presence of n-CdS with high resistivity excludes the presence of a strong field at the edge of the metal contact and forms p-n transition, parallel to the barrier, Al/p-CdS. The conductivity of the tunnel transparent dielectric Al_2O_3 present on the surface of aluminum is much higher than the conductivity of an inversely biased p-n junction and most of the applied external voltage drops on the p-n junction. Direct current-voltage characteristic structure of Al/p-CdS/n-CdS is almost identical to the current-voltage characteristics of p-n junctions. In this case, the current through the structure increased exponentially with increased applied voltage. In the course of temperature dependence of the slopes of the lines $\ln I \sim U$ can be divided into two temperature ranges.

The increase in the forward voltage observed at the beginning section of the VAC with a large slope corresponds to when one current flow mechanism is replaced by another. The reverse saturation current was two orders of magnitude smaller than the current through the tunnel-transparent oxide layer of Al_2O_3 and 10^{-10} cm^{-2} for the high temperature region ($T > 250$ K). The activation energy of the saturation current in this case was 0.9 eV, which was less than the barrier and the current was not purely thermal emission, and thus the corresponding emission-recombination mechanism.

Film sandwich structures of CdS-Al in the presence of an intermediate Al_2O_3 layer showed the effect of switching to a steady state conduction, which in some approximation can be regarded as the prebreakdown and breakdown after state. After the breakdown condition, studies showed that at $T = 80$ K, there can be two types of conductivity — low and high. These states were also reproduced. The physical nature of the state can only be understood by studying the mechanisms of conduction film systems at different stages of change. The Ha basis for the measurement of volt-farad characteristics data of samples established the presence of conduction due to the presence of reverse bias p-n junctions. There was found to be high hole concentration (10^{21} cm^{-3}), characteristic of the conducting state.

In type 1 $Zn_{1-x}Cd_xS$/p-CdS windows, a 0.15 μm-thick ZnCdS film was first deposited on an Al substrate. This was then dipped in a $CdCl_2$ methanol solution for about 30 s to improve the conductivity, then dried with an infrared lamp, and then rinsed in deionized water. This was followed by an additional deposition of 0.05 μm CdS thin film to complete the window fabrication. In a type 2 p-CdS/$Zn_{1-x}Cd_xS$ window, a 0.15 μm thick p-CdS film, sandwiched between two 0.4 μm-thick $Zn_{1-x}Cd_xS$ films, was first deposited by CBD on an Al substrate.

4. Conclusion

We investigated the preparation of ZnCdS nanoparticles in a micro emulsion system. The $Zn_{1-x}Cd_xS$ ($0 \leqslant x \leqslant 1$) films deposited from solution and the sensitivity conditions of these films have been determined. The obtained results showed that when controlling the ionic composition and HT conditions, one can control the properties of $Zn_{1-x}Cd_xS$ ($0 \leqslant x \leqslant 1$) films.

The chemical composition and the degree of crystallization are not the only determining factors for the difference in photoelectric properties, as this can also be attributed to the nature and the concentration distribution of recombination centers and trapping levels. The direct current-voltage characteristic structure of Al/p-CdS/n-CdS is almost identical to the current-voltage characteristics of p-n junctions. Volt-farad characteristics of samples established the presence of conduction due to the presence of reverse bias p-n junctions. In the following order, CdTe/CdS/$Zn_{1-x}Cd_xS$ structures have 75% or slightly higher quantum efficiency in the 400–850 nm wavelength region.

References

[1] P.Babu, M.V. Reddy, N. K. Revathi, T.R. Reddy. Effect of pH on the physical properties of $ZnIn_2Se_4$ thin films grown by chemical bath deposition. *Journal of Nano- and Electronic Physics*, **3**, P. 85–91 (2011).

[2] E. Bacaksiz, S. Aksu, I. Polat, S. Yilmaz, M. Altunbas. The influence of substrate temperature on the morphology, optical and electrical properties of thermal evaporated ZnSe thin films. *Journal of Alloys and Compounds*, **487**, P. 280–285 (2009).

[3] A.S. Abdinov, M.A. Jafarov, N.M. Mekhtiev. Photosensitivity of the CdSSe films near the JR region Proc. of SPIE, **4340**, P. 107–111 (2000).

[4] A. Dumbrava. Zinc sulfide fine particles obtained at low temperature. *Chalcogenide Letters*, **6**(9), P. 437–443 (2009).

[5] J. Yang, G. Wang, H. Liu, X. Chen. Controlled synthesis and characterization of ZnSe nanostructures via a solvothermal approach in a mixed solution. *Mater. Chem. Phys.*, **115**, P. 204–208 (2009).

[6] J.B. Chaudhari, N.G. Deshpande, Y.G. Gudage, A. Ghosh, V.B. Huse, R. Sharma. Studies on growth and characterization of ternary $CdS_{1-x}Se_x$ alloy thin films deposited by chemical bath deposition technique. *Applied Surface Science*, **254**, P. 6810–6816 (2008).

[7] A. Apolinar-Iribe, M.C. Acosta-Enriquez, M.A. Quevedo-Lopez, R. Ramirez-Bon, A. De-Leon, S.J. Castillo. Acetylacetone as complexing agent for CdS thin films grow chemical bath deposition. *Chalcogenide Letters*, **8**, P. 77–82(2011).

[8] L.Y. Chen, D.L. Zhang, G.M. Zhai, J.B. Zhang. Comparative study of ZnSe thin films deposited from modified chemical bath solutions with ammonia-containing and ammonia free precursors. *Materials Chemistry and Physics*. **120**, P. 456–460 (2010).

[9] V.E. Lashkarev, A.V. Lyubchenko, M.K. Sheynkman. *Nonequilibrium processes in photoconductors*. N. Dumka, Kiev, 264 p. (1991).

[10] S.M. Nair, P.K. Nair, R.A. Zingaro. Chemical bath deposition of photosensitive CdS and CdSe thin films and their conversion to n-type for solar cell application. *Proc.SPIE*, **2531**, P. 254–264 (1995).

[11] T.P. Kumar, P.D. Ramesh, B.J. Abaraj. Effect of ethylenediamine tetraacetic acid concentration on the photoluminescence behavior of CdZnS thin films. *Chalcogenide Letters*, **8**, P. 207–212 (2011).

[12] Gopakumar, N.P. Anjana, P.P. Vidyadharan. Chemical bath deposition and characterization of CdSe thin films for optoelectronic applications. *J. Materials Sci.*, **45**, P. 6653–6656 (2010).

[13] W.C. Song, J.H. Lee. Growth and characterization of $Zn_xCd_{1-x}S$ films prepared by using chemical bath deposition for photovoltaic devices. *Journal of the Korean Physical Society*, **54**, P. 1660–1665 (2009).

[14] D. Patidar, K.S. Rathore, N.S. Saxena, T.P. Sharma. Determination of optical and electrical properties of ZnSe thin films. *Journal of Modern Physics*, **55**, P. 3041–3047 (2008).